Eur. Phys. J. Appl. Phys. **28**, 173–178 (2004)
DOI: 10.1051/epjap:2004182

THE EUROPEAN PHYSICAL JOURNAL APPLIED PHYSICS

Non-uniformity of temperatures along nanotubes in hot reactors and axial growth

T. Laude[a] and Y. Matsui

National Institute for Materials Science, Advanced Materials Laboratory, Namiki 1-1, Tsukuba, Ibaraki, 305-0044, Japan

Received: 17 July 2003 / Received in final form: 12 May 2004 / Accepted: 15 June 2004
Published online: 30 August 2004 –

Abstract. Non-uniformity of temperatures appears as a general rule in hot nanofiber synthesis reactors, where local variations of the balance between long-range radiative heat exchanges and short-range conductive heat exchanges are driven by size and composition of structures. Metal particles larger than a few tens of nanometer are radiation captors, when fiber bodies thinner than 10 nm are transparent. We note that typical gradient lengths correspond remarkably well to usual length of nanotubes (micron range), and increase with fiber radius. For anisotropically radiating reactors as well as for furnace-type reactors, difference between radiative and conductive environments allows temperature intervals as high as several hundred degrees. Practically, axial thermal gradients arise by fiber attachment to a metallic particle, eventually at each tip (ideally with different sizes or compositions), or by attachment to a hot wall (electrode, supporting substrate, or target). The resulting thermal gradients are unusually stiff, typically 10 $\mathrm{K}\,\mu\mathrm{m}^{-1}$. We show that local temperature evolution in early stage of nucleation is triggered by dimension of attached particle(s). We show that a diffusion flux of adatoms induced by the axial thermal gradient is quantitatively consistent with a feeding flux, as measured for different reactors. In addition, we notice that the spontaneous minimization of free energy at fiber tip is such that a temperature drop favors axial extension.

PACS. 61.46.+w Nanoscale materials: clusters, nanoparticles, nanotubes, and nanocrystals – 82.60.Qr Thermodynamics of nanoparticles – 81.16.-c Methods of nanofabrication and processing

1 Introduction

The growth of nanometer-large fibers, like nanotubes, eludes understanding of growth process, firstly because of poor ability in stating local growth conditions. Early considerations stated the catalytic importance of nanosized metallic particles at nanotube tip [1]. It has been shown the ability of such particles, probably liquid at temperature involved, to accumulate carbon atoms, and add them to fiber either by surface or volume diffusion [2]. In the mean time, the hypothesis of open-end growth was proposed, supported by post-synthesis observations of opened tubes [3], as well as by stabilizing lip-lip interactions [4]. However extensive experimental work showed that the presence of open-ended tubes is no general rule. It remains to explain the favoring of growth in one direction. Obviously, strong planar atomic organization, such as found for carbon and boron nitride (BN), favors tubular growth. However, nanofibers form for diverse compositions and crystallographies, including amorphous.

In reactors involving temperatures in the range 900–4000 K, non-uniformity of temperature is a factor of general validity. An original work for arc discharge reactors, considering thermal fluctuations of nanotube tips, has showed discordance between global reactor temperature and growth temperature of nanotubes [5]. We modeled temperature along a nanotube with simplified black body hypothesis in an earlier work [6]. One particularity of nanometer-sized material is that radiative exchange is conditioned by dimension and composition. Indeed, black body absorption and emission apply only to matter larger than attenuation length of thermal radiations, which is in the nanometer order for metals but over the micron order for dielectrics. In consequence, dimension and composition have the ability to trigger radiative exchanges, so that long-range radiative exchanges compete with short-range conductive exchanges. For a mix of structures with different thermal properties, this results in non-uniformity of temperatures on very short distances.

In this paper, we propose a modelisation of this effect for a nanofiber in conditions suitable with different types of synthesis reactors. Formalism relies on a simple one-dimensional equation of heat diffusion, but is largely dependant on local conditions around the nanofiber and on reactor configuration. In terms, we aim to hint the role of the axial thermal gradient in nanofiber growth. We describe an axial flux of adatom due to the thermal gradient. In addition, we remark that fast temperature drop at tip favors the growth. We believe thermal gradient can

[a] e-mail: thomaslaude@yahoo.fr

both provide feeding fluxes and favor fiber extension, in accordance with measured growth speed, and other experimental knowledge.

2 Modeling of temperatures for a nanofiber inside reactor

2.1 Configuration hypothesizes for the modeling

With laser ablation method [4], tubes are thought to grow in plume plasma, and are obtained attached to metallic particles at tips. Growth speed was estimated in the range 0.6–5.1 $\mu\mathrm{m\,s^{-1}}$ [7]. With non-ablative laser heating method [8], BN fibers grow attached to a hot h-BN target, and tubes have a liquid boron particle at the other tip. Growth speed was estimated of order 10 $\mu\mathrm{m\,s^{-1}}$ in the first second of the growth, and rapidly decreasing later. Arc discharge method is specific for providing both cases, of growth with attachment to graphite electrode without metallic particle [9], or without attachment to electrode but with metallic particle [10]. CVD methods, which involve lower temperatures (under 1200 K), provide growth with attachment to a hot substrate, a metallic particle being also attached at the other tip or at attachment with substrate. Growth speed was estimated much lower, in the range 0.03–0.014 $\mu\mathrm{m\,s^{-1}}$, but for nanotube of diameter 60 to 240 nm. Growth speed was proposed proportional to inverse of diameter [11]. In flash CVD process, carbon micro-trees growing from electrodes were obtained with a growth speed of 3.3 $\mu\mathrm{m\,s^{-1}}$ [12].

To modelize any of these methods, we consider a fiber, which may be a nanotube, single or multi-walled, a nanotube bundle, or even a plain fiber. (Only effective fiber section matters for thermal modeling.) This fiber is attached at $z = 0$ to a thermal reservoir (furnace wall, target surface, electrode surface, supporting substrate, or large particle), large enough for its temperature, T_{tr}, not to be affected by the rest of the structure. The other tip is attached at $z = h$ to a metallic particle, which may be of negligible dimensions (absent) (Fig. 1). Fiber diameter is typically in the range 0.5–500 nm. Particle size is typically in the range 3–500 nm. Composition and crystallography of the structure are not specified as they do not affect the formalism of the thermal modeling. (We suppose any crystallization latent heat flux at growing tip much smaller than radiations from the tip.) However for numerical applications, the fiber may be supposed solid, typically graphite or h-BN, and eventually amorphous, and the metallic particle(s) may be supposed liquid or amorphous, typically Fe, Co, Ni, B, ...

We consider a reactor such that hot radiative solid angle is closed completely (as in CVD, and laser ablation furnaces) or only partially (growth near a target, an electrode, or on a supporting substrate). But in any case, we consider a uniform temperature for the radiator, T_r. (Absorption by an eventual quartz or silicate tube is neglected.) Gas environment is supposed at uniform temperature T_g around the structure. (It is at same temperature than the radiator only if the structure is close enough to the radiator.) Such uniform environment hypothesizes neglect the thermal influence of other structures (for instance, that of a nanotube forest).

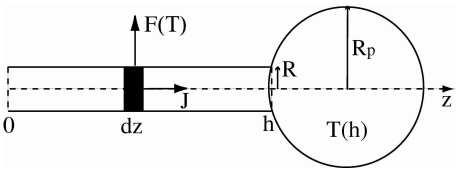

Fig. 1. Notations. Attachment to a thermal reservoir at 0. Particle at h.

We consider that radial temperature across fiber, as well as across nano-metallic particle, is closely uniform, so that unidimensional formalism is justified. We also consider steady state. Indeed, typical time for temperature stabilization by thermal diffusion along fiber is h^2/η (η thermal diffusivity, $\approx 10^{-5}$ $\mathrm{m^2\,s^{-1}}$ typically). Even for fast growing nanotube (say 10 $\mu\mathrm{m\,s^{-1}}$), temperatures stabilize after a negligible extension of fiber length. Also, environment around fiber is stable, or at least such that its change during h^2/η is negligible, even if fiber is moving in reactor chamber[1].

Finally, we do not consider a difference of thermal accommodation coefficient, ε_g, between fiber and particle(s). (We suppose a majority of inert molecules in gas phase.) It would be necessary to do so if a majority of gas molecules condenses instead of bouncing on metal particles.

2.2 Modeling

Temperatures along fiber axis follow the unidimensional equation of heat diffusion,

$$\frac{\mathrm{d}^2T}{\mathrm{d}z^2} - \frac{1}{kR_e}F(T) = \frac{C}{k}\frac{\mathrm{d}T}{\mathrm{d}t}. \qquad (1)$$

(F external heat fluxes, k axial thermal conductivity, C thermal capacity, R_e ratio of effective section surface to section outer perimeter. $R_e = R/2$ for a plain cylindrical fiber.) k is closely constant at high temperatures (although temperature dependent at low temperature [13]). For layered materials like carbon and BN, k is close to the in-plane conductivity of the material. (For

[1] Some experimental observations indicate that temperature stability of environment is necessary during fiber growth. Most reactor producing long tubes allow long stability in the nucleation zone: CVD (hours), non-ablative laser heating (minutes near target), DC arc discharge (seconds near the electrodes), laser ablation (seconds in plume). On the opposite, fiber synthesized in unstable conditions (laser ablation reactor without furnace, or arc discharge reactor away from electrodes or with AC current) tubes are less than few hundreds microns long. For instance, with AC discharge, temperature is stable for only $\approx 2 \times 10^{-2}$ s, corresponding to fiber length ≈200 nm (with growth speed 10 $\mu\mathrm{ms^{-1}}$). This is compatible with the measurements of H. Zeng, L. Zhu, G. Hao, and R. Sheng, Carbon **36**, 259 (1998).

graphite, $k \approx 250\ \mathrm{J\,s^{-1}\,m^{-1}\,K^{-1}}$ at 2000 K [14]. For h-BN, $k \approx 60\ \mathrm{J\,s^{-1}\,m^{-1}\,K^{-1}}$ at 300 K [15].)

On surface of fiber or particle, heat loss is due to exchanges with surrounding gas, and with distant radiating walls:

$$F(T) = \varepsilon\delta\sigma T^4 - A_r\varepsilon_r\varepsilon\delta\sigma T_r^4 - A_g(T_g - T). \qquad (2)$$

For analytical treatment, the fourth power of temperature in equation (2) is cumbersome. We use linearized expression valid for $T \sim T_r$: $F(T) \sim aT - b$, with $a = 4\varepsilon\delta\sigma T_r^3 + A_g$ and $b = \varepsilon\delta\sigma T_r^4(\varepsilon_r A_r + 3) + A_g T_g$.

[T_r temperature of radiating walls, A_r ratio of the solid angle closed by radiating walls as seen from surface, ε_r total emittance of radiating walls, ε total emittance[2] of surface, δ "thickness opacity" coefficient (defined below), T_g gas temperature, A_g gas coefficient (defined below), σ the Stefan-Boltzman constant.] Exchanges by latent heat along fiber body are reasonably neglected.

Incident radiation [second term in Eq. (2)] may be due to furnace walls, target surface, electrode surface, or supporting substrate, ... A_r is essential for it separates reactors in two types: for closed furnace $A_r \approx 1$, but for hemispherical radiators (target, electrode, supporting substrate) $A_r \approx 0.5$. (This difference is enhanced by ε_r, because in closed furnace multiple reflections cause $\varepsilon_r \approx 1$.)

Because of nanometer scale, radiation absorption is limited by fiber or particle thickness. δ is roughly equal to smallest value between 1 and αd, where d is thickness, and $1/\alpha$ is the attenuation length of incident radiation (averaged on wavelength and supposed constant on temperatures) [16]. δ is an essential thermal factor for it strongly depends on size and composition. For a metal, $1/\alpha$ is typically a few tens of nanometers. Hence, over such dimension, a metallic particle is fully submitted to radiative exchange ($\delta = 1$). On the opposite, for dielectrics, $1/\alpha$ can be well over the micron range. Hence, true insulator nanofibers, like BN fibers, are transparent ($\delta = 0$), whatever their thickness. Metallic (typically carbon) nanofibers are versatile. A thin metallic nanotube is transparent. However, thick metallic bundles or nanotubes (10 to 100 nm) are submitted to radiative exchange to some extend. (For boron, metallic behavior may be expected at high temperature.) {Emitted radiation [first term in Eq. (2)] is symmetrical to incident radiation, by virtue of Kirchhoff law.}

Conductive heat exchange with gas [third term in Eq. (2)] is proportional to energy transferred during gas-surface collisions. [$A_g = (3/2)\varepsilon_g k_B J_g$ (gas supposed mono-atomic for illustration) with ε_g thermal accommodation coefficient, k_B the Boltzman constant, J_g molecular flux from gas ($J_g = (2\pi m_g k_B T_g)^{-1/2} P_g$, with m_g molecular mass, P_g gas pressure).] ε_g is similar to δ in that it depends on composition and temperature (of gas and surface). Unfortunately, experimental measurements of this coefficient are scarce [17]. Typically ε_g varies from 1 to 10^{-2}. For an inert gas at high temperature, ε_g is small because of molecular bouncing. But for a surface attractive to gas molecules (close to condensation), $\varepsilon_g \approx 1$.

[2] According to Kirchhoff's law, total absorptance is equal to total emittance ε (measurable), provided that incident radiation spectrum is proportional to that of a black body near temperature T and independent of incident direction in the solid angle closed by radiating walls. ε is supposed constant on the range of temperatures.

2.3 Results of the modeling

2.3.1 Gradient length

Temperature along a fiber [solution of Eq. (1)] varies with the typical length ("gradient length"):

$$z_0 = \left(\frac{kR_e}{a}\right)^{1/2}. \qquad (3)$$

Typically, z_0 is in the order of tens of μm. It increases with R_e. One consequence is that gradient length of nanotube bundles is longer than that of individual tubes. It should be noted that this corresponds well to typical lengths of nanotubes obtained experimentally. z_0 is also influenced weakly by k (factor 2 between carbon and BN) and by a number of configuration factors through a.

2.3.2 Maximum temperature interval of a reactor

Temperatures are restricted to an interval between temperature reached for heat exchange with gas only, T_g, and temperature reached for heat exchange with radiator only, $(\varepsilon_r A_r)^{1/4} T_r$. These two values only depends on reactor configuration, not on structure configuration. Two cases are of particular interest:

- Reactor type 1: (fiber growing on electrodes in arc discharge reactor, or on target in a non-ablative laser heating reactor) $T_r = T_g$ because a hot thermal gas layer embeds growth zone. However, $(\varepsilon_r A_r)^{1/4} < 1$, first because $A_r < 1$ (radiating electrodes or target do not close the solid angle), and also because $\varepsilon_r < 1$ (a typical value for ceramic walls being 0.8). In that case, the maximum temperature interval allowed by the reactor is $[1 - (\varepsilon_r A_r)^{1/4}]T_r$.
- Reactor type 2: (CVD or laser ablation, inside a furnace) $T_r > T_g$ because of conductive heat loss through glass tube/gas and of convective loss in carrier gas. However, $(\varepsilon_r A_r)^{1/4} \approx 1$ because of furnace enclosure. In contrast with previous case, radiation is warmer than surrounding gas. The maximum temperature interval allowed by the reactor is simply $T_r - T_g$, the value of T_g being dependent on configuration and position in the furnace, but eventually in the order of hundreds degrees, in particular near furnace borders.

2.3.3 Equilibrium temperatures of fiber and particle

Temperature of the fiber far from any attachments T_{eq} is such that $F(T_{eq}) = 0$. With linearized expression of F,

$$T(z) = \frac{(T_{tr} - T_{eq})\left(\cosh\left(\frac{h-z}{z_0}\right) + c\ \sinh\left(\frac{h-z}{z_0}\right)\right) + c\ \left(T^p_{eq} - T_{eq}\right)\sinh\left(\frac{z}{z_0}\right)}{\cosh\left(\frac{h}{z_0}\right) + c\ \sinh\left(\frac{h}{z_0}\right)} + T_{eq}, \quad (4)$$

$T_{eq} \approx b/a$. Similarly, temperature of a hypothetical isolated particle in gas is $T^p_{eq} \approx b_p/a_p$. [The temperature of a particle at the tip of a long fiber is $(T_{eq} + cT^p_{eq})/(1+c)$, where c depends mainly on relative size of particle and fiber. See below.] In contrast, T_{tr} is defined by the configuration. (For example, $T_{tr} = T_g$ for attachment to a hot wall where thermal gas layer embeds growth zone.) T_{eq}, T^p_{eq} and T_{tr} are nested in reactor interval.

2.3.4 Thermal gradient

Solution of equation (1) is straightforward, considering T_{tr} at $z = 0$, and the equality of heat fluxes at $z = h$: $-2\pi R R_e k[\mathrm{d}T/\mathrm{d}z]_{z=h} = 4\pi R_p^2 F_p(T(h))$. (Index p for particle at $z = h$.) With the linearized form of F and F_p, the general expression of the thermal gradient is

see equation (4) above

where $c = (2R_p^2 a_p)/(R z_0 a)$ is particle/fiber ratio for thermal exchange power. If $T_{tr} > T_{eq}$, temperature is mostly decreasing from $z = 0$ to $z = h$. However if $T_{eq} < T^p_{eq}$, temperature rise locally near $z = h$. (Symmetrically for $T_{tr} < T_{eq}$.)[3]

2.3.5 Evolution of particle temperature during the growth

Temperature of the particle at $z = h$ is simply found in equation (4). It is constantly cooling/warming during the growth, from T_{tr} to $(T_{eq} + cT^p_{eq})/(1+c)$. This illustrates c, as a geometrical parameter switching between particle-induced temperature to fiber-induced temperature.

In beginning of the growth (short h), the presence of a large and opaque particle at $z = h$ is a condition for a fast temperature drop. Indeed, $[\mathrm{d}T_{z=h}/\mathrm{d}h]_{h=0} = -c(T_{tr} - T^p_{eq})/z_0$. This is a fraction c of an average "particle-induced gradient", little dependent on fiber material.

[3] There are two specific cases for $T(z)$. Firstly, if no particle or if the particle at $z = h$ has same thermal properties than fiber, $T^p_{eq} = T_{eq}$. If in addition $T_{tr} = T_g$, gradient is conditioned by the opacity of the material. (If transparent, $\delta = 0$, $T_{eq} = T_g$.) For $c \approx 1$, or near $z = h$ for a long fiber, the gradient is a simple exponential, $T(z) \sim (T_{tr} - T_{eq})\exp(-z/z_0) + T_{eq}$, not affected by tube extension (independent of h), and $T(h)$ follows this simple exponential variation. Secondly, if fiber is transparent, $T_{eq} = T_g$. If in addition $T_{tr} = T_g$, gradient is conditioned by opacity of the particle. (If particle is transparent, $T^p_{eq} = T_g$.) For $c \approx 1$, $T(z) \sim (T^p_{eq} - T_{tr})\sinh(z/z_0)\exp(-h/z_0) + T_{tr}$. In contrast with previous case, $T(z)$ varies (exponentially) with tube extension (but $T(h)$ still follows a simple exponential variation).

3 Example application: arc discharge method, growth on electrodes

We consider a configuration compatible with arc discharge method carbon SWNT, growth on electrodes. A transparent nanotube is attached to a hot electrode at $z = 0$ and to an opaque metal particle at $z = h$ (Reactor type 1). We use default numerics: $P_g = 3 \times 10^4$ Pa, $m_g = 6.64 \times 10^{-26}$ kg ($\mathrm{H_e}$), $\varepsilon_r = 0.8$, $\varepsilon_g = \varepsilon^p_g = 0.1$, $k = 250$ SI, $R_e = 0.25$ nm, $R_p = 10$ nm, $A_r = 0.5$, $T_{tr} = T_g = T_r = 3000$ K, $\varepsilon = 0.4$, $\varepsilon^p = 0.6$, $\delta = 0$, $\delta^p = 1$. It results: $J_g \approx 2.28 \times 10^{26}\ \mathrm{m^{-2}\,s^{-1}}$, $A_g = A^p_g = a \approx 4.73 \times 10^2$ SI, $a^p \approx 4.15 \times 10^3$ SI, $b \approx 1.42 \times 10^6$ SI, $b^p \approx 1.08 \times 10^7$ SI.

Gradient length $z_0 \approx 11$ μm with default numerics. However, if $R_e = 12.5$ nm ($R \approx 25$ nm bundle of nanotubes) $z_0 \approx 81$ μm. This corresponds well to typical lengths of nanotubes obtained experimentally. z_0 is little influenced by radiator (electrode) temperature T_r (Fig. 2a). On the opposite, the interval ΔT reached between tips when fiber is long is strongly dependant on radiator temperature (Fig. 2b). $\Delta T/z_0$ increases from 0.1 to 20 $\mathrm{K\,\mu m^{-1}}$, from 1000 K to 4000 K.

The fiber being transparent, its temperature far from any attachment is that of the gas ($T_{eq} = T_g$). The temperature of a hypothetical individual particle in gas is very low ($T^p_{eq} \approx 2600$ K). However, the actual temperature of the particle at $z = h$ for a long fiber is a fraction of that ($(T_{eq} + cT^p_{eq})/(1+c) \approx 2907$ K, $c \approx 0.3$). Figure 2c shows temperature along fiber for different h, and temperature of the particle at $z = h$ with increasing h. Temperature is decreasing from $z = 0$ to $z = h$, and stiffer near $z = h$. The temperature of the particle at $z = h$ is decreasing during the growth, and this decrease is faster in early stage of the growth. (Temperature at a given z is actually increasing during the growth.) In these circumstances, temperature gradient may strongly influence the early stage of growth. This effect is strongly dependant on particle dimension at $z = h$ (Fig. 2d). (Decrease of opacity for small particle is not considered.)

4 Extension to other configurations

In previous example, we could have considered an opaque (large) fiber attached to the electrode. In that case, a temperature gradient exists, even without particle (in which case $T(h)$ tends to T_g with h). However the gradient is flat near $z = h$, and the decrease of temperature at $z = h$ in early stage of growth is slow. In these circumstances, temperature gradient cannot influence the early stage of growth. (Unless fiber first grows thin.)

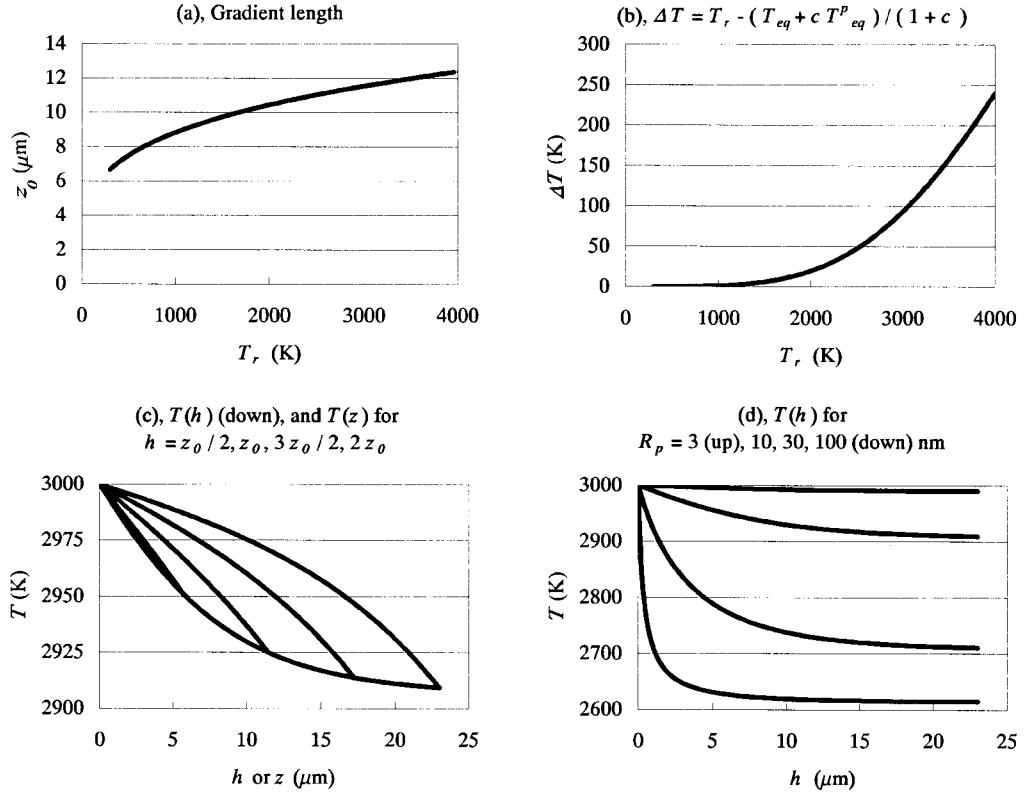

Fig. 2. Thermal gradient values for arc discharge reactor, SWNT grown attached to electrodes at temperature $T_{tr} = T_g = T_r = 3000$ K and with an opaque particle at $z = h$. (a) Gradient length z_0 as function of T_r. As the fiber is transparent, the variation is purely due to conductive exchanges. (b) Temperature interval between tips for long SWNT, as function of T_r. (c) $T(h)$ (down), and $T(z)$ for several h. (d) Variation of $T(h)$ with particle radius. Large particle is essential to induce a fast temperature drop in the beginning of the growth. (Default numerics.)

If fiber is grown in gas phase, without attachment to a hot wall but only to particle(s), we have to consider $T_{tr} = T^p_{eq}$ fixed at one tip (a particle is large enough). The case of attachments at opposite tips to respectively, an opaque and a transparent particle is of particular interest. Their temperature tendency to respectively T^p_{eq} and T_g causes a very fast temperature evolution in the early stage of the growth. This can be obtained by particles different in size, or in composition if several catalysts are used. (The advantage of using a mix of two metals as catalysts is common knowledge in laser ablation method.)

In previous example, as well as for fiber grown in gas phase, if all parts of the structure are transparent, no gradient is possible. In that case, temperature is uniform and equal to T_g.

5 Discussion: Some kinetic consequences of a stiff thermal gradient

5.1 Surface diffusion along fiber due to a static gradient

At high temperature, adatoms (or admolecules) migrate along fiber surfaces. Axial diffusion flux is caused by adatom concentration gradient $J_n = -D_n \mathrm{d}n/\mathrm{d}z$ [2], or by thermal gradient $J_T = -D_T \mathrm{d}T/\mathrm{d}z$. [These fluxes are correlated, n being determined by (temperature dependent) transition rates fiber-adatom and adatom-gas, and by impinging flux from gas.]

(Case n uniform.) The mobility of adatoms along fiber surface is determined by distance for an adatom to lose its direction (inertia) by interaction with surface sites, λ. ($\lambda = \nu\tau$, with τ mean travel time, and ν average surfacial speed.) We consider that adatoms simply jump between neighboring sites, hence λ is the inter-site distance, and $\nu = \nu_0 \exp(-\delta E_d / k_B T)$, where δE_d is activation energy for surface diffusion. [However, for most reactors, $k_B T (\approx 0.1{-}0.3$ eV for $T = 1000{-}3000$ K) is of same order than δE_d (≈ 0.13 eV). Therefore the exponential coefficient is close to 1 (close to the case of a free 2D gas), and λ is higher than the inter-site distance.]

Diffusion flux induced by thermal gradient is easily expressed as a function of the physical parameters. The flux crossing a segment of length $2\pi R$ from one side is $2Rn\nu$. (Maxwellian distribution of speeds.) Considering that this flux is roughly due to adatoms from regions $z \pm \lambda$, this leads to $D_T = 2Rn\lambda \mathrm{d}\nu/\mathrm{d}T$. Using above expression for ν and assuming ν_0 proportional to temperature, $\mathrm{d}\nu/\mathrm{d}T \approx 2\nu/T$.

It follows

$$D_T = \frac{4Rn\lambda\nu}{T}. \quad (5)$$

J_T is quantitatively consistent with a feeding flux, considering experimental fiber growth speeds. In addition, lineic density of atoms in fiber being proportional to R^2 (plain fiber), it accounts for a decrease of growth speed with fiber radius as $1/R$. For instance, for a non-ablative laser synthesis, with numerics (SI units): $R \approx 1.3 \times 10^{-9}$, $n \approx 10^{18}$ (arbitrary high up to site concentration), $\lambda \approx 2.5 \times 10^{-10}$, $\nu \approx 1.6 \times 10^3$ [$\approx (2k_BT/m)^{1/2}$], $T \approx 2 \times 10^3$, $\mathrm{d}T/\mathrm{d}z \approx 10^7$, we find $J_T \approx 10^7$ s^{-1}. This corresponds well to experimental growth speed 10 μm s^{-1}, considering a bi-layered tube. For CVD, with numerics: $R \approx 20 \times 10^{-9}$, $n \approx 10^{18}$, $\lambda \approx 2.5 \times 10^{-10}$, $\nu \approx 10^3$, $T \approx 10^3$, $\mathrm{d}T/\mathrm{d}z \approx 5 \times 10^5$, we find $J_T \approx 10^7$ s^{-1}. This also corresponds to experimental growth speed (0.05 μm s^{-1}) considering a plain tube.

It should be noted that feeding rate by thermal diffusion at growing tip is diminishing (exponentially) with increasing h (as does $\mathrm{d}T/\mathrm{d}z$). In addition, for a given reactor, a specific R is imposed by the competition between variation of J_T (proportional to R) and of flux needed (proportional to R_e^2).

5.2 Consequences of a temperature drop at fiber tip

Length increase at fiber growing tip is controlled by local minimization of free energy $\mathrm{d}E - T_{eq}^{tip}\mathrm{d}S = (1 - T_{eq}^{tip}/T(h))\mathrm{d}E$, where $\mathrm{d}E \approx Nk_B\mathrm{d}T + \mathrm{d}U$, U including structural energies: latent heat or surface energy[4]. (Number of atoms N, and volume held constant. Reversible case.) This minimization causes length increase if length-dependent terms can be minimized. Length dependent terms are thermal energy, surface energy, and some latent heat (ex: length increase favor planar bounds over strained bonds for carbon or BN). If thermal term is dominant in this last minimization, fiber tip roughly follows a path of minimization of temperature. Thermal term is expected dominant at least for isotropic materials (amorphous in particular). {The change in which fiber length is increased of one atom (highest temperature drop), causes a typical thermal energy drop of 0.01 eV [with numerics (SI units): $N \approx 2 \times 10^6$, $\mathrm{d}T = (1/c_h)\mathrm{d}T/\mathrm{d}h$, where $c_h \approx 2 \times 10^{11}$ is the lineic density of atoms in a bi-layered tube, and $\mathrm{d}T/\mathrm{d}h \approx 10^7$]. With thermal gradient ranging from 1 to 100 K μm^{-1}, the thermal energy drop ranges from 0.001 to 0.1 eV.}[5]

The authors would like to thank Oleg Louchev for helping to the thermal modeling, Ken-Ichi Ohshima and Bernard Jouffrey for Ph.D. supervision.

References

1. A. Oberlin, M. Endo, T. Koyama, J. Cryst. Growth **32**, 335 (1976)
2. O. Louchev, Y. Sato, H. Kanda, Phys. Rev. E **66**, 011601 (2002)
3. S. Ijima, P.M. Ajayan, T. Ichihashi, Phys. Rev. Lett. **69**, 3100 (1992)
4. T. Guo, P. Nikolaev, A.G. Rinzler, D. Tomanek, D.T. Colbert, R.E. Smalley, J. Phys. Chem. **99**, 10694 (1995)
5. V.H. Crespi, Phys. Rev. Lett. **82**, 2908 (1999)
6. T. Laude, Ph.D. thesis, University of Tsukuba, March 2001; École Centrale Paris, March 2001 (Contact the author for a copy.)
7. A. Puretzky, H. Schittenhelm, X. Fan, M. Lance, L. Allard, D. Geohegan, Phys. Rev. B **65**, 245425 (2002)
8. T. Laude, Y. Matsui, A. Marraud, B. Jouffrey, Appl. Phys. Lett. **76**, 3239 (2000)
9. T.W. Ebbesen, H. Hiura, J. Fujita, Y. Ochiai, S. Matsui, K. Tanigaki, Chem. Phys. Lett. **209**, 83 (1993)
10. S. Iijima, T. Ichihashi, Nature **363**, 603 (1993)
11. C.J. Lee, S.C. Lyu, Y.R. Cho, J.H. Lee, K.I. Cho, Chem. Phys. Lett. **341**, 245 (2001)
12. P. Ajayan, J. Nugent, R. Siegel, B. Wei, Ph. Kohler-Redlich, Nature **404**, 243 (2000)
13. J. Hone, M. Whitney, C. Piskoti, A. Zettl, Phys. Rev. B **59**, R2512 (1999)
14. Y.S. Touloukian, R.W. Powell, C.Y. Ho, P.G. Klemens, *Thermophysical properties of matter* (IFI/Plenum, New York, Washington, 1970), Vol. 2, Thermal conductivity, p. 41
15. Advanced Ceramic Corporation, Measurements on pyrolitic BN, 22557 West Lunn Road, Cleveland, Ohio USA 44149 (unpublished)
16. J. Costa, P. Roura, J.R. Morante, E. Bertran, J. Appl. Phys. **83**, 7879 (1998)
17. L.B. Thomas, *Fundamentals of Gas-Surface Interactions, proceedings of the Symposium of December 14-16 1966, San Diego, California*, edited by H. Saltsburg, J.N. Smith, M. Rogers (Academic Press, New York and London, 1967), p. 346

[4] Atoms follow minimization path only if tip explores spontaneously configurations in an interval of time consistent with the growth (by local movements or global vibrations of the tip). Obviously, such exploration is made easier if tip is liquid, or if it has a high density of mobile atoms (adatoms, ...).

[5] For illustration, we can consider a kinetic mechanism of extension ("thermal machine") for an idealized case. For fiber without particle at tip, and supposing $\mathrm{d}U$ negligible, spontaneous exploration of morphologies is caused by surface diffusion. With time, adatoms accumulate at tip (fiber length increases), because when atoms move to tip, tip temperature decrease and backward moves are less probable. Such flux towards tip is very similar to the static flux described in IV.A, except that the change of average speed for one atom jump is now determined by length increase as $(1/c_h)\mathrm{d}\nu/\mathrm{d}h$. This leads to $J = -(2Rn/c_h)(\mathrm{d}\nu/\mathrm{d}T)\mathrm{d}T/\mathrm{d}h$. This is quantitatively comparable to the flux obtained in IV.A. Therefore such mechanism is consistent with experimental growth speeds.